consist in calling the reader's attention to those points which seem of greatest importance. Let us consider, first, the tests of the circular cylinder.

The sudden appearance of the cross-wind force at $r = 0 \cdot 5$ seems so definitely established that mere coincidence is doubtful. Unfortunately, no study of the smoke flow was made in this range, so it is not known whether there is an abrupt change in the flow pattern to account for the phenomenon.

Beyond the ratio $r = 0 \cdot 5$, the cross-wind force increases steadily through quite a range in which there is practically no variation in drag, the value of the latter remaining constant between $r = 0 \cdot 5$ and $2 \cdot 0$. With values of r greater than $2 \cdot 0$ the drag increases and the maximum ratio of lift to drag ($7 \cdot 8$) is attained when $r = 2 \cdot 5$ approximately. It is noted that the drag coefficient at this point is almost identical with that of the stationary cylinder.

The high values of C_{CW} result, of course, from the very unsymmetric velocity distribution around the cylinder. The smoke photographs (Figs. 15, 16 and 17) clearly depict the gradual distortion of the symmetrical flow pattern with increasing rotation and the building up of a very high velocity region opposite one of considerably reduced velocity. Thus the rotation produces the same sort of velocity distribution as does camber in the case of an airfoil. The greater dissymmetry of this flow, as compared to that about an airfoil, is undoubtedly due to the fact that the proportionate increase and decrease of the free stream velocity is considerably augmented by the rotation.

In connection with the variation of drag, the following points are noted :—The smoke photographs show that at small values of r the groups of streamlines from the two sides of the cylinder do not diverge so markedly as is the case with the motionless cylinder. This accounts for the first reduction of drag. Through the range in which C_D remains constant, although C_{CW} increases rapidly, there must be balance of the changes in the flow pattern around the upstream and down-stream halves of the cylinder. With further increase of rotative speed, it is seen (Fig. 17) that the streamlines from the high velocity side wrap farther and farther around the cylinder. It seems probable that as the stagnation point moves back along the low velocity side, it will finally meet and merge with the point at which the two groups of streamlines reunite. A completely different type of flow will naturally result, and the rapid increase of drag and reduction in the rate of increase of lift are its characteristics.

The fact that the power input is smaller with moving than stationary air indicates a reduction of air friction. This would be expected as the relative velocity of air to cylinder is reduced, around most of the circumference, by the rotation.

The characteristics of the cross cylinder, throughout the range covered, were very irregular. The relatively high power required to rotate this model prevented the reaching of high values of r. However, in the upper portion of the speed range, the data were fairly consistent, and as an L/D ratio of $5 \cdot 5$ was attained at $r = 1 \cdot 8$, it would not be at all surprising if the maximum L/D ratio for this cylinder were found to be larger than that for the circular one.

The hysteresis effect found at low values of r has received no explanation, but it may be mentioned that the lower values (dashed curve in Fig. 7) were observed when the rotative speed was increasing, air speed being held constant; as the rotative speed was reduced, the points on the upper curve were obtained.

While the curve of C_{CW} *vs.* r, for the cross cylinder, is rather erratic, if the portion between $r = 1 \cdot 0$ and $1 \cdot 8$ were projected as far as the r axis, the intersection would occur at $r = 0 \cdot 5$. The slope of this section of the curve is identical with that of the first portion of the corresponding curve for the circular cylinder.

The power consumption of the cross cylinder is greater in moving than in still air at values of r greater than $1 \cdot 0$, but less at smaller ratios.

The results from the tests of the compound strut cover a

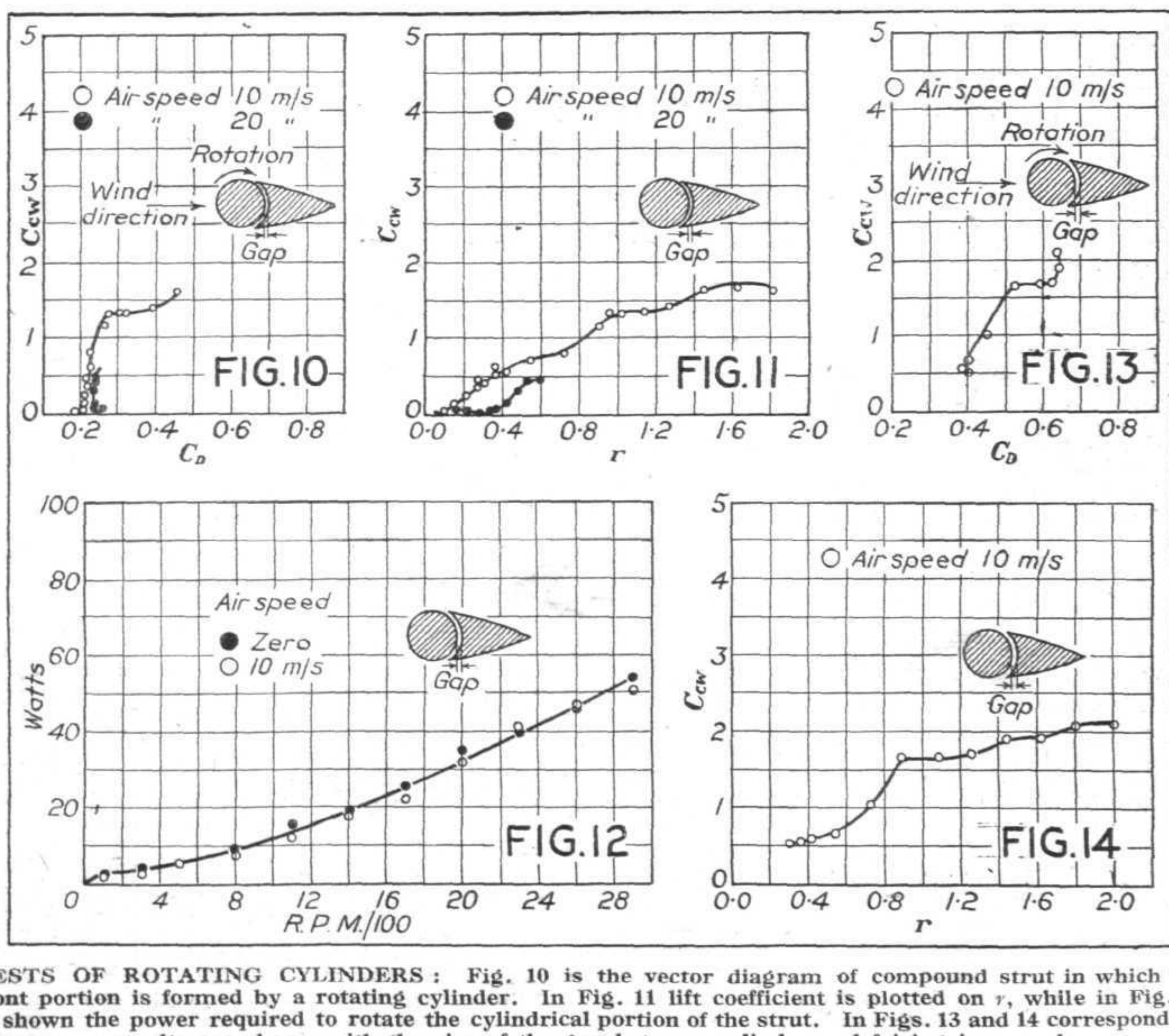

TESTS OF ROTATING CYLINDERS : Fig. 10 is the vector diagram of compound strut in which the front portion is formed by a rotating cylinder. In Fig. 11 lift coefficient is plotted on r, while in Fig. 12 is shown the power required to rotate the cylindrical portion of the strut. In Figs. 13 and 14 corresponding results are shown with the size of the gap between cylinder and fairing increased.